Spectroscopic detection of C IV λ1548 in a galaxy at z = 7.045: implications for the ionizing spectra of reionization-era galaxies

Daniel P. Stark, Gregory Walth, Stéphane Charlot, Benjamin Clément, Anna Feltre, Julia Gutkin, Johan Richard, Ramesh Mainali, Brant Robertson, Brian Siana, et al.

Monthly Notices
of the
ROYAL ASTRONOMICAL SOCIETY

MNRAS **454,** 1393–1403 (2015) doi:10.1093/mnras/stv1907

Spectroscopic detection of C IV λ1548 in a galaxy at $z = 7.045$: implications for the ionizing spectra of reionization-era galaxies

Daniel P. Stark,[1⋆] Gregory Walth,[1] Stéphane Charlot,[2] Benjamin Clément,[3] Anna Feltre,[2] Julia Gutkin,[2] Johan Richard,[3] Ramesh Mainali,[1] Brant Robertson,[1] Brian Siana,[4] Mengtao Tang[1] and Matthew Schenker[5]

[1]*Steward Observatory, University of Arizona, 933 N Cherry Ave, Tucson, AZ 85721, USA*
[2]*Sorbonne Universités, UPMC-CNRS, UMR7095, Institut d'Astrophysique de Paris, F-75014 Paris, France*
[3]*Centre de Recherche Astrophysique de Lyon, Universite Lyon 1, 9 Avenue Charles Andre, F-69561 Saint-Genis Laval Cedex, France*
[4]*Department of Physics & Astronomy, University of California, Riverside, CA 92507, USA*
[5]*PDT Partners, LLC, 1745 Broadway, New York, NY 10019, USA*

Accepted 2015 August 16. Received 2015 August 14; in original form 2015 April 23

ABSTRACT

We present Keck/MOSFIRE observations of UV metal emission lines in four bright ($H = 23.9$–25.4) gravitationally lensed $z \simeq 6$–8 galaxies behind the cluster Abell 1703. The spectrum of A1703-zd6, a highly magnified star-forming galaxy with a Lyα redshift of $z = 7.045$, reveals a confident detection of the nebular C IV λ1548 emission line (unresolved with full width at half-maximum <125 km s^{-1}). UV metal emission lines are not detected in the three other galaxies. At $z \simeq 2$–3, nebular C IV emission is observed in just 1 per cent of UV-selected galaxies. The presence of strong C IV emission in one of the small sample of galaxies targeted in this paper may indicate that hard ionizing spectra are more common at $z \simeq 7$. The total estimated rest-frame equivalent width of the C IV doublet and C IV/Lyα flux ratio are comparable to measurements of narrow-lined AGNs. Photoionization models show that the nebular C IV line can also be reproduced by a young stellar population, with very hot metal-poor stars dominating the photon flux responsible for triply ionizing carbon. Regardless of the origin of the C IV, we show that the ionizing spectrum of A1703-zd6 is different from that of typical galaxies at $z \simeq 2$, producing more H ionizing photons per unit 1500 Å luminosity ($\log(\xi_{\rm ion}/{\rm erg^{-1}\ Hz}) = 25.68$) and a larger flux density at 30–50 eV. If such extreme radiation fields are typical in UV-selected systems at $z \gtrsim 7$, it would indicate that reionization-era galaxies are more efficient ionizing agents than previously thought. Alternatively, we suggest that the small sample of Lyα emitters at $z \gtrsim 7$ may trace a rare population with intense radiation fields capable of ionizing their surrounding hydrogen distribution. Additional constraints on high-ionization emission lines in galaxies with and without Lyα detections will help clarify whether hard ionizing spectra are common in the reionization era.

Key words: galaxies: evolution – galaxies: formation – galaxies: high-redshift – cosmology: observations.

1 INTRODUCTION

Our understanding of galaxy growth in the first billion years of cosmic time has developed rapidly in the last five years following a series of deep imaging campaigns with the infrared channel of the Wide Field Camera 3 (WFC3/IR) on board the *Hubble Space Telescope* (*HST*). Deep WFC3/IR exposures have delivered more than ∼1500 galaxies photometrically selected to lie between ≃0.5 and 1 Gyr after the big bang (e.g. Bouwens et al. 2015) and the first small samples of galaxies within the first 0.5 Gyr of cosmic time (e.g. Zheng et al. 2012; Coe et al. 2013; Ellis et al. 2013; Oesch et al. 2014; Zitrin et al. 2014; Atek et al. 2015).

These studies demonstrate that the $z \gtrsim 6$ galaxy population is different from well-studied samples at $z \simeq 2$–3. The UV luminosities, star formation rates (SFRs) and stellar masses tend to be lower at $z \simeq 6$ (e.g. Smit et al. 2012; McLure et al. 2013; Schenker et al. 2013a; Bouwens et al. 2014; Duncan et al. 2014; Grazian et al. 2015; Salmon et al. 2015), the sizes are smaller (e.g. Oesch et al. 2010; Ono et al. 2013; cf. Curtis-Lake et al. 2014), and the UV

⋆ E-mail: dpstark@email.arizona.edu

Table 1. High-redshift galaxies targeted with our Keck/MOSFIRE observations. Details on observations and reduction are presented in Section 2. The final column provides the reference to the paper where the galaxy was first discussed in the literature. The magnitude of A1703-23 is from the *H*-band filter on Subaru/MOIRCS, while the others are from WFC3/IR imaging in the H_{160} filter. For A1703-zd4, the '†' symbol marks the fact that we are sensitive to C IV over only a portion of the redshift range suggested by the photometry. References: [1] Bradley et al. (2012); [2] Richard et al. (2009). A1703-23 also appears in Zheng et al. (2009) as 'A1703-id1'.

Source	RA	Dec.	z_{spec}	z_{phot}	H_{160}	μ	UV lines targeted	Ref
A1703-zd1a	13:14:59.418	+51:50:00.8	–	6.6-6.9	23.9	9.0	C IV, He II, O III]	[1]
A1703-zd4	13:15:07.189	+51:50:23.6	–	7.0-9.3	25.4	3.1	Lyα, C IV†	[1]
A1703-zd6	13:15:01.007	+51:50:04.4	7.043	–	25.9	5.2	N IV], C IV, He II, O III]	[1]
A1703-23	13:15:01.469	+51:48:26.5	5.828	–	23.8	3.0	C III]	[2]

continuum colours are bluer (e.g. Wilkins et al. 2011; Finkelstein et al. 2012; Rogers, McLure & Dunlop 2013; Bouwens et al. 2014). Specific star formation rates at $z \gtrsim 6$ are large, indicating a rapidly growing young stellar population (e.g. Stark et al. 2013; González et al. 2014; Salmon et al. 2015).

The emission line properties of early galaxies also appear different. Large equivalent width Lyα emission is more common among $z \simeq 6$ galaxies than it is in similar systems at $z \simeq 3$ (e.g. Stark, Ellis & Ouchi 2011; Curtis-Lake et al. 2012). The strongest rest-frame optical lines ([O III], Hα) are more difficult to characterize since they are situated at 3-5 μm, where thermal emission from the atmosphere impedes detection with ground-based facilities. Nevertheless, progress has been achieved by isolating galaxies at redshifts in which the [O III] or Hα line contaminates the *Spitzer*/IRAC broad-band filters. In the last several years, this technique has been used to characterize the equivalent width distribution of Hα in $3.8 < z < 5.0$ galaxies (Shim et al. 2011; Stark et al. 2013) and [O III]+Hβ in $z \simeq 6.6$–6.9 (Smit et al. 2014, 2015) and $z \simeq 8$ (Labbé et al. 2013) galaxies, revealing that typical [O III] and Hα rest-frame equivalent widths of $z \simeq 4$–7 galaxies are significantly larger than among similar systems at $z \simeq 2$. The population of extreme emission line galaxies (rest-frame EW = 500–1000 Å), relatively rare among $z \simeq 1$–2 galaxies (e.g. Atek et al. 2011; van der Wel et al. 2011; Maseda et al. 2014), appears to be ubiquitous at $z \simeq 7$ (Smit et al. 2014, 2015).

The common presence of extreme optical line emission holds clues as to the physical nature of $z \gtrsim 7$ galaxies. Recent work has demonstrated that optical line ratios among $z \simeq 2$ galaxies require an ionizing radiation field that is harder than that in $z \simeq 0$ galaxies (e.g. Kewley et al. 2013; Steidel et al. 2014), consistent with a blackbody with mean effective temperatures of 50 000–60 000 K. The increased incidence of extreme line emitters at $z \simeq 7$ with respect to $z \simeq 2$ may suggest that the net ionizing field is powered by even hotter stars at $z \simeq 7$. Such a finding would indicate that galaxies are very efficient ionizing agents throughout the tail end of the reionization era and would have important implications for the nature of the massive stars within $z \simeq 7$ galaxies.

Further progress in our understanding of the radiation field of early galaxies will only come from detailed spectroscopy. Prior to *James Webb Space Telescope* (*JWST*), spectroscopic observations of $z \gtrsim 7$ galaxies will be limited to the rest-frame far-ultraviolet (FUV) window. The FUV contains several emission lines with higher ionization potential than in the rest-frame optical (i.e. C IV, He II), providing a valuable probe of the ionizing spectrum. While nebular emission from these species is rarely seen among luminous star-forming galaxies, they have been identified more commonly in metal-poor galaxies with low masses (Erb et al. 2010; Christensen et al. 2012; Stark et al. 2014). Such systems also commonly show strong emission from the O III] λλ1661, 1666 and C III] λλ1907, 1909 intercombination lines (Garnett et al. 1995, 1997, 1999; Erb et al. 2010; Bayliss et al. 2014; James et al. 2014; Stark et al. 2014).

Little is currently known about whether FUV spectra of galaxies are in the reionization era. But with the discovery of an increasing number of bright $z \gtrsim 6$ galaxies (e.g. Bowler et al. 2014; Bradley et al. 2014), this is now beginning to change. Recently, Stark et al. (2015) reported tentative C III] detections in two galaxies with previously confirmed redshifts ($z = 6.029$ and 7.213) from Lyα. Here we build on this progress with an exploration of the strength of high-ionization emission features (C IV λλ1548, 1551 and He II λ1640) in a small sample of $z \simeq 7$ UV-selected galaxies using the MOSFIRE (McLean et al. 2012) spectrograph on the Keck I telescope. We report the detection of strong nebular C IV λ1548 emission in the spectrum of A1703-zd6, a spectroscopically confirmed galaxy at $z = 7.045$. The total C IV equivalent width is greater than that in existing samples of $z \simeq 2$ metal-poor star-forming galaxies (Christensen et al. 2012; Stark et al. 2014) but is similar to that seen in narrow-lined AGNs (Hainline et al. 2011; Alexandroff et al. 2013), pointing to a hard radiation field in one of the most distant known galaxies.

Other galaxies on the MOSFIRE mask include a spectroscopically confirmed Lyα emitting galaxy at $z = 5.828$ (Richard et al. 2009) and A1703-zd1a, a photometrically selected galaxy thought to lie in the range $z \simeq 6.6$–6.9 with *Spitzer*/IRAC colours (Bradley et al. 2012; Smit et al. 2014) indicating extreme [O III]+Hβ emission in the rest-frame optical and a bright z-band dropout (A1703-zd4 in Bradley et al. 2012) with photometry suggesting a redshift in the range $z = 7.0$–9.3. No strong emission lines are seen in any of these systems (Table 1).

The plan of the paper is as follows. In Section 2 we describe the MOSFIRE observations. The spectra are discussed in Section 3, and the photoionization modelling procedure is described in Section 4. We explore implications of our findings in Section 5 and summarize the results in Section 6. We adopt a Λ-dominated, flat Universe with $\Omega_\Lambda = 0.7$, $\Omega_M = 0.3$ and $H_0 = 70\,h_{70}\,km\,s^{-1}\,Mpc^{-1}$. All magnitudes in this paper are quoted in the AB system (Oke & Gunn 1983).

2 KECK/MOSFIRE OBSERVATIONS

Near-infrared (NIR) spectroscopic observations of Abell 1703 were carried out with MOSFIRE (McLean et al. 2012) on the Keck I telescope on 2014 April 11 UT. The spectroscopic observations were taken using the *YJ* grating with the *J*-band filter, which has a resolution of $R = 3318$ and covers a wavelength range of $\lambda = 1.15$–1.35 μm. A mask was created for Abell 1703 with 1.0 arcsec width slits. Individual exposures were 120 s with two position dithers of 3.0 arcsec having a total integration time of 2.6 h. The average

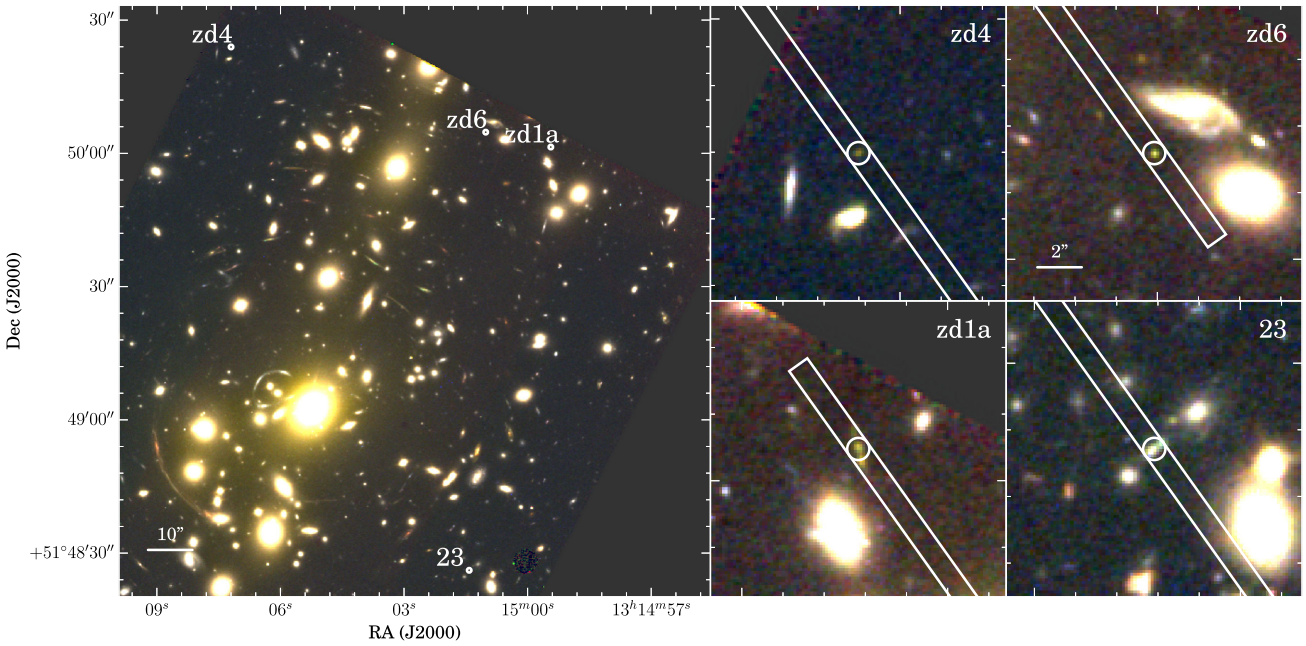

Figure 1. Overview of the Keck/MOSFIRE *J*-band observations of four gravitationally lensed galaxies at $5.8 < z < 7.0$ in the field of Abell 1703. Positions of the galaxies are overlaid on the *HST* colour image (z_{850}, J_{125}, H_{160} bands) of the cluster. The right-hand panel shows a zoomed-in view. Information on the galaxies and MOSFIRE spectra is presented in Section 3.

seeing throughout the observation was 0.80 arcsec (full width at half-maximum, FWHM). The four $z \gtrsim 5$ galaxies on the mask are shown in Fig. 1.

The spectra were reduced using the MOSFIRE Data Reduction Pipeline (DRP). The MOSFIRE DRP performs the standard NIR spectroscopic reduction, flat-fielding, wavelength calibration, sky subtraction and cosmic ray removal to produce 2D spectra. The instrumental response and telluric absorption across the *J* band were corrected using long-slit observations of a standard star. The absolute flux calibration was performed using a star placed in the mask of the science field with *HST* ACS (*F*850*LP*) and WFC3/IR (*F*125*W*, *F*160*W*) photometry. We calculate the factor necessary to scale the observed flux of the star to the observed *F*125*W* magnitude and then apply this absolute flux correction factor to the standard star spectrum. The 1D spectra were extracted with 1.1, 1.4 and 1.8 arcsec (6, 8, 10 pixels) apertures. The apertures are chosen to be larger than the atmospheric seeing and the size of the lensed systems. In the following analysis, we used the 1.1 arcsec pixel aperture unless stated otherwise. The uncertainty on the MOSFIRE wavelength calibration is $\simeq 0.1$ Å in the 1D extracted spectra.

3 RESULTS

In the following, we discuss the physical properties of each of the four galaxies that form the basis of this study and report the detections and non-detections arising from the MOSFIRE spectra.

3.1 A1703-zd6

A1703-zd6 is a bright ($H = 25.9$) *z*-band dropout first identified in Bradley et al. (2012). A spectroscopic redshift ($z = 7.045$) was achieved via detection of Lyα at 9780 Å (Schenker et al. 2012). The absolute UV magnitude is found to be $M_{\rm UV} = -19.3$ after correcting for the source magnification ($\mu = 5.2$).

The MOSFIRE *J*-band spectrum of A1703-zd6 covers 1.1530–1.3519 μm providing spectral coverage between 1433 and 1680 Å in the rest frame, enabling constraints on the strength of N IV], C IV, He II and O III]. The Lyα redshift (Schenker et al. 2012) allows us to predict the window over which these lines will be located. In doing so, we must account for the velocity offset between Lyα and the other FUV lines. We expect the N IV], C III] and O III] doublets to trace the systemic redshift (Vanzella et al. 2010; Stark et al. 2014a) and Lyα to be redshifted between 0 and 450 km s^{-1} with respect to the systemic redshift. The C IV λ1549 doublet is a resonant line and may also appear redshifted with respect to the other FUV metal lines.

The C IV doublet is easily resolved by MOSFIRE at $z \simeq 7$. If C IV traces gas at the same redshift as Lyα ($z = 7.045 \pm 0.003$), we would expect C IV λ1548 to be located between 1.2450 and 1.2460 μm and C IV λ1550 between 1.2471 and 1.2481 μm. As can be seen in the 2D spectrum shown in Fig. 2, C IV λ1548 is confidently detected at 1.2458 μm, which is within the window defined by the Schenker et al. (2012) Lyα detection. C IV λ1550 is also likely detected at 1.2474 μm. A skyline redwards of the line makes determination of the exact centroid difficult. The C IV λ1548 line flux is $4.1 \pm 0.6 \times 10^{-18}$ erg cm^{-2} s^{-1} using the 1.8 arcsec aperture which maximizes the S/N. Determination of the C IV λ1550 flux is considerably more difficult because of the neighbouring skyline. We measure a line flux of $3.8 \pm 0.9 \times 10^{-18}$ erg cm^{-2} s^{-1} bluewards of the skyline. This includes contribution from a broad blue wing which is visible in the 1D extracted spectrum and corresponds to diffuse emission in the 2D spectrum. Given the low S/N of the line, it is unclear whether this broad extension is actually associated with the observed line. We thus place a conservative lower bound on the flux of the emission feature ($2.1 \pm 0.6 \times 10^{-18}$ erg cm^{-2} s^{-1}) by masking the diffuse emission bluewards of the line centre. A deeper integration will be required to improve the S/N of this tentative feature, but in the rest of the paper we will adopt $2.1–3.8 \times 10^{-18}$ erg cm^{-2} s^{-1} as the

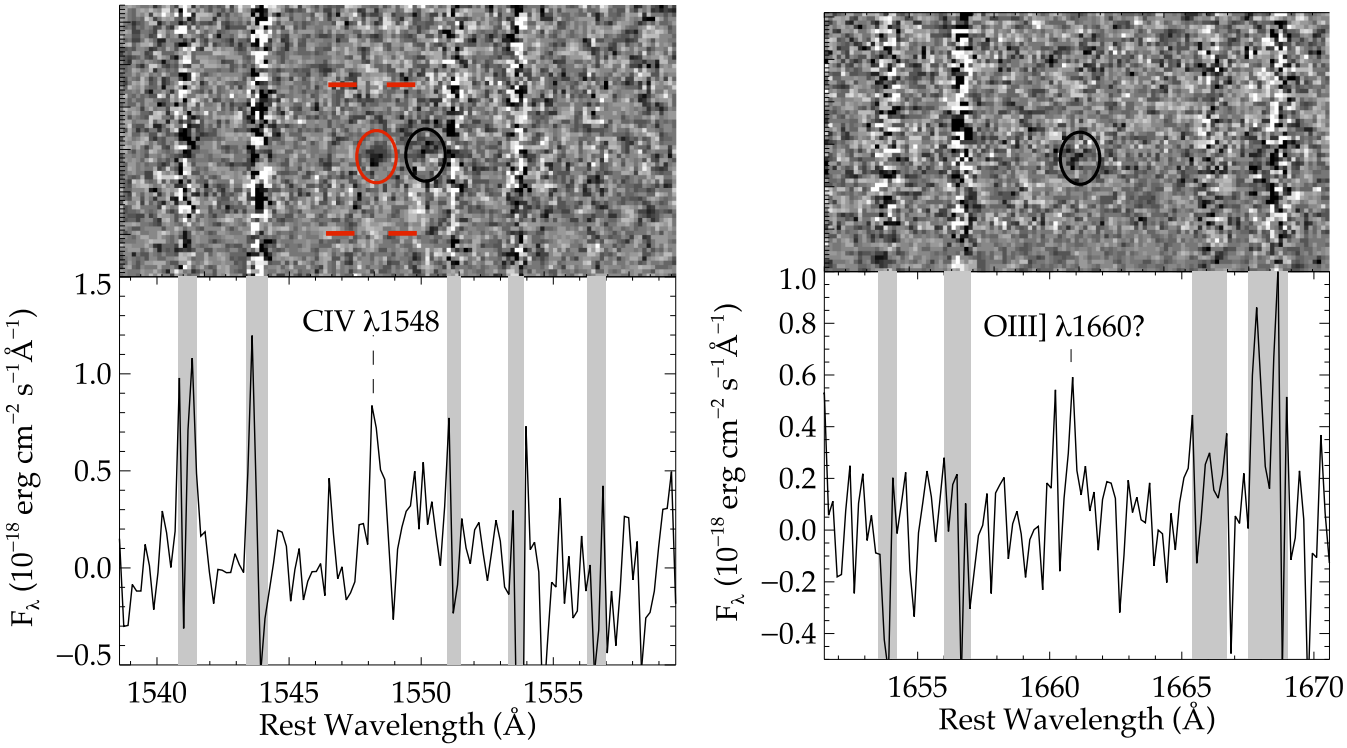

Figure 2. Keck/MOSFIRE *J*-band spectrum of the gravitationally lensed $z_{\mathrm{Ly}\alpha} = 7.045$ galaxy A1703-zd6. The spectroscopic redshift was known prior to MOSFIRE observations from Lyα emission (Schenker et al. 2012). Top panels show the two-dimensional (unsmoothed) spectra with black showing positive emission. The red oval identifies the emission feature at the rest-frame wavelength expected for C IV λ1548. The characteristic negative emission from the dither pattern is demarcated by red horizontal lines. Black ovals highlight the expected location of C IV λ1550 (left-hand panel) and O III] λ1660 (right-hand panel). The one-dimensional extracted spectra are shown in the lower panels. Vertical grey swaths indicate regions of elevated noise from OH skylines.

possible line flux range for this component. When conducting photoionization modelling later in the paper, we will focus our analysis on the more robust detection of C IV λ1548. Taking into account the seeing and the fraction of the galaxy covered by the MOSFIRE slit, we estimate that an aperture correction of a factor of 1.2 must be applied to the line flux for accurate equivalent width measurements. Applying this correction, we derive rest-frame equivalent widths of 19.9 ± 3.6 and 18.1 ± 4.6 Å for the C IV λ1548 and C IV λ1550 components, respectively. We note that for the lower bound we place on C IV λ1550, the rest-frame equivalent width is 9.8 Å. The equivalent width uncertainties reported here and below include the contribution from galaxy magnitude errors (typically 0.1 mag). The observed spectral FWHM of C IV λ1548 (5.2 Å) is identical to the FWHM of nearby skylines indicating that the line is narrow and unresolved with a velocity FWHM of $\lesssim$125 km s^{-1}.

To predict the wavelengths of the O III] $\lambda\lambda$1660, 1666 doublet, we consider Lyα velocity offsets ($\Delta v_{\mathrm{Ly}\alpha}$) between 0 and 450 km s^{-1}, consistent with observations of $z \simeq 2$ galaxies (Tapken et al. 2007; Steidel et al. 2010). Under these assumptions, the O III] λ1660 line will lie between 1.3341 μm ($\Delta v_{\mathrm{Ly}\alpha} = 450$ km s^{-1}) and 1.3361 μm ($\Delta v_{\mathrm{Ly}\alpha} = 0$ km s^{-1}). An emission feature is visible in this spectral window at 1.3358 μm (Fig. 2). We tentatively identify this line as O III] λ1660. After accounting for the aperture correction, the measured line flux ($1.8 \pm 0.7 \times 10^{-18}$ erg cm^{-2} s^{-1}) implies a rest-frame equivalent width of 9.8 ± 3.9 Å.

Since C IV and Lyα are both resonant transitions, O III] λ1660 provides the only constraint on the systemic redshift. From the peak flux of emission feature, we estimate a redshift of $z_{\mathrm{sys}} = 7.0433$. The Ly$\alpha$ velocity offset that would be implied by this tentative detection, $\Delta v_{\mathrm{Ly}\alpha} = 60$ km s^{-1}, suggests that Lyα is emerging close to systemic redshift. A more robust detection is required to verify the Lyα velocity offset. But we note that this measurement would be consistent with both Lyα emitting galaxies at $z \simeq 2$ (Tapken et al. 2007; McLinden et al. 2011; Hashimoto et al. 2013). Such small velocity offsets appear to be more common at higher redshifts (Schenker et al. 2013b; Stark et al. 2015), consistent with the rising fraction of Lyα emitting galaxies with redshift over $3 < z < 6$ (Stark et al. 2011). As discussed in Choudhury et al. (2014), existence of small Lyα velocity offsets at $z \gtrsim 6$ reduces the IGM neutral hydrogen fraction required to explain the rapid attenuation of Lyα over $6 < z < 7$. The resonant C IV λ1548 line is slightly more redshifted (with a peak close to 120 km s^{-1} from the possible O III] λ1660 feature) than Lyα. The tentative difference in velocity between C IV and Lyα would not be surprising since the covering fraction and kinematics of the neutral hydrogen (which scatters Lyα photons) are likely to be very different from the highly ionized gas which scatters C IV (e.g. Steidel et al. 2010).

At $z = 7.0433$, the O III] λ1666 is located on top of a strong skyline at 1.340 μm (Fig. 2) and is not detected in the MOSFIRE spectrum. We also do not detect He II λ1640 or N IV] $\lambda\lambda$1483, 1487. Flux and rest-frame equivalent width limits (2σ) are provided in Table 2. Non-detection of He II and N IV] is consistent with the emission line spectra of $z \simeq 1.5$–3 metal-poor dwarf galaxies (Christensen et al. 2012; Stark et al. 2014). In these systems, the FUV metal lines (C IV, C III], O III]) are typically much stronger than He II and N IV]. The 2σ upper limit on the He II-to-Lyα flux ratio (<0.07) is nevertheless consistent with the spectrum of BX 418 ($f_{\mathrm{He\,II}}/f_{\mathrm{Ly}\alpha} = 0.03$), a metal-poor $z = 2.3$ galaxy discussed in detail in Erb et al. (2010). A deeper *J*-band spectrum of A1703-zd6 would be required to determine if He II is present at a similar flux as BX 418.

Table 2. Emission line properties of the $z_{Ly\alpha} = 7.045$ galaxy A1703-zd6 (Bradley et al. 2012). An aperture correction of a factor of 1.20 must be applied to the emission line fluxes if computing line luminosities. The '†' symbol next to Lyα notes that this flux measurement is from Schenker et al. (2012). Measurement of the line flux of the C IV λ1550 component is challenging. We place a lower limit on its flux and rest-frame equivalent width of 2.1 $\times 10^{-18}$ erg cm^{-2} s^{-1} and 9.8 Å, respectively. See discussion in Section 3.1 for details. The O III] λ1666 emission line is obscured by a skyline. The equivalent widths include the aperture correction and are quoted in the rest frame. The limits are 2σ.

Line	λ_{rest} (Å)	λ_{obs} (Å)	Line flux (10^{-18} erg cm^{-2} s^{-1})	W_0 (Å)
Lyα†	1215.67	9780	28.4 ± 5.3	65 ± 12
N IV]	1483.3	–	<3.6	<15.7
–	1486.5	–	<4.3	<19.0
C IV	1548.19	12 457.9	4.1 ± 0.6	19.9 ± 3.6
–	1550.77	12 473.5	3.8 ± 0.9	18.1 ± 4.6
He II	1640.52	–	<2.1	<11.4
O III]	1660.81	13 358.3	1.8 ± 0.7	9.8 ± 3.9
–	1666.15	–	–	–

3.2 A1703-zd1a

A1703-zd1a is a very bright ($H = 23.9$) z-band dropout. After correcting for its lensing magnification ($\mu = 9.0 \pm 4.5$; Bradley et al. 2012), the absolute magnitude ($M_{UV} = -20.6$) of A1703-zd1a is found to be identical to $L^{\star}_{UV}$ at $z \simeq 6.8$ (Bouwens et al. 2015). The UV slope ($\beta = -1.4$; Smit et al. 2014) is redder than average for $L^{\star}_{UV}$ z-drops (Bouwens et al. 2014). Measurement of the *Spitzer*/IRAC [3.6]−[4.5] colour reveals a strong flux excess in [3.6], suggestive of strong [O III]+Hβ line contamination (Smit et al. 2014). This likely places the galaxy in the redshift range $z = 6.6$–6.9 where [O III]+Hβ is in [3.6] and Hα is between the [3.6] and [4.5] filters. In this redshift range, the MOSFIRE J-band spectrum is sensitive to emission from C IV, He II and O III]. Since both components of C IV and O III] are resolved, there are up to five emission lines which could be visible in the spectrum.

Examination of the MOSFIRE spectrum reveals no features as strong as the C IV λ1548 line in A1703-zd6. In regions between skylines, the 5σ upper limit to the line flux is 3.0×10^{-18} erg cm^{-2} s^{-1}. Given the seeing, slit width and source size, we estimate that an aperture correction of a factor of 1.27 is required for comparison of line fluxes to the total continuum flux densities. Applying this correction factor to the line flux limit, we derive a 5σ rest-frame equivalent width limit of 2.3 Å, considerably lower than that seen in the spectrum of A1703-zd6. The spectrum is sensitive to C IV over $6.4 < z < 7.7$, covering the entire redshift range suggested by the photometric redshift. Given the prominent optical line emission implied by the *Spitzer*/IRAC colours, we might have expected to detect C IV or O III]. Among $z \simeq 2$–3 extreme optical line emitters, C IV and O III] equivalent widths can reach values greater than our sensitivity limits (e.g. Stark et al. 2014). A key difference between A1703-zd1a and the lower redshift extreme line emitters is the UV slope. The red UV slope of A1703-zd1a may point to moderate dust content and significant attenuation of the UV lines.

3.3 A1703-zd4

A1703-zd4 is another bright ($H_{160} = 25.4$) z-band dropout galaxy identified in Bradley et al. (2012). The broad-band spectral energy distribution (SED) is best fitted by a redshift of $z = 8.4$ with acceptable solutions ranging between $z = 7.0$ and 9.3 (Bradley et al. 2012). After taking into account the source magnification ($\mu = 3.1$), the absolute magnitude of A1703-zd4 is $M_{UV} = -20.6$ at its best-fitting photometric redshift. The J-band MOSFIRE spectrum is sensitive to Lyα over the redshift range $8.5 < z < 10.1$ and C IV over $6.4 < z < 7.7$.

We have visually examined the spectrum for potential emission features. While several low-S/N features are present, no definitive redshift identification is possible with the current spectrum. Conservatively assuming a line width of 10 Å (twice the value of the C IV λ1548 line in A1703-zd6) and 1.1 arcsec aperture along the slit, we find that typical 5σ line flux limits are 2.6×10^{-18} erg cm^{-2} s^{-1} in between OH skylines. Taking into account the seeing, slit width and galaxy size, we compute an aperture correction of a factor of 1.21. Applying this correction to the line flux limit and using the J_{125}-band magnitude from Bradley et al. (2012) as the continuum flux density at 1.15–1.35 μm, we derive a rest-frame equivalent width limit of ≃6 Å for regions between OH lines. With the resolution provided by MOSFIRE, the incidence of OH lines is minimized, but none the less roughly 40 per cent of the J-band spectral window is still impacted by skylines so it is of course possible that an emission line from A1703-zd4 is obscured by a bright skyline.

Additional spectroscopy will help clarify the redshift of A1703-zd4, as the current J-band exposure only samples a portion of the photometric redshift distribution function. A Y-band spectrum would extend the Lyα coverage down to the redshift range $7.0 < z < 8.2$, while an H-band spectrum of A1703-zd4 would extend the redshift range over which FUV metal lines are detectable.

3.4 A1703-23

A1703-23 was identified as a bright ($H = 23.75$) i-band dropout and spectroscopically confirmed in Richard et al. (2009). Lyα was detected in an optical spectrum at 8300.5 Å implying a redshift of $z = 5.828$, consistent with expectations from the SED. Richard et al. (2009) measure a Lyα flux of 2.5×10^{-17} erg cm^{-2} s^{-1}. After correcting for the magnification factor estimated by Richard et al. (2009), $\mu = 3$, the UV absolute magnitude of A1703-23 is found to be $M_{UV} = -21.7$, corresponding to a 1.6–2.0$L^{\star}_{UV}$ galaxy at $z \simeq 5.9$ (Bouwens et al. 2015). Similar to A1703-zd1a, the UV spectral slope of A1703-23 ($\beta = -1.5$) is redder than typical i-band dropouts. Since the continuum is not detected in the optical spectrum, we estimate the Lyα equivalent width from the broad-band flux measurements. We use the UV spectral slope to convert the J-band flux to a continuum flux at the wavelength of Lyα. Following this procedure, we estimate a rest-frame equivalent width of $W_{Ly\alpha} = 10.3$ Å for A1703-23.

Using the Lyα spectroscopic redshift, we predict the observed wavelengths over which the C III] doublet will be located. Studies at lower redshift demonstrate that C III] tends to trace the systemic redshift (Stark et al. 2014). Allowing for the characteristic Lyα velocity offset of 0–450 km s^{-1} with respect to the systemic redshift, we predict that [C III] λ1907 will lie between 1.2999 and 1.3019 μm and C III] λ1909 will be located between 1.3013 and 1.3033 μm. The flux ratio of [C III] λ1907 to C III] λ1909 is set by the electron density in the gas traced by doubly ionized carbon. In high-redshift galaxies, observations indicate [C III] λ1907/C III]1909 flux ratios in the range 1.2–1.6 (Hainline et al. 2009; James et al. 2014).

As can be seen in the 2D spectrum (Fig. 3), no strong emission lines are detected. There is a skyline that would likely obscure C III] λ1907 at the very edge of the spectral window (1.3018–1.3019 μm), corresponding to Lyα velocity offsets of −7 to 15 km s^{-1}. There is a much weaker skyline at 1.3000–1.3003 μm, corresponding to Lyα

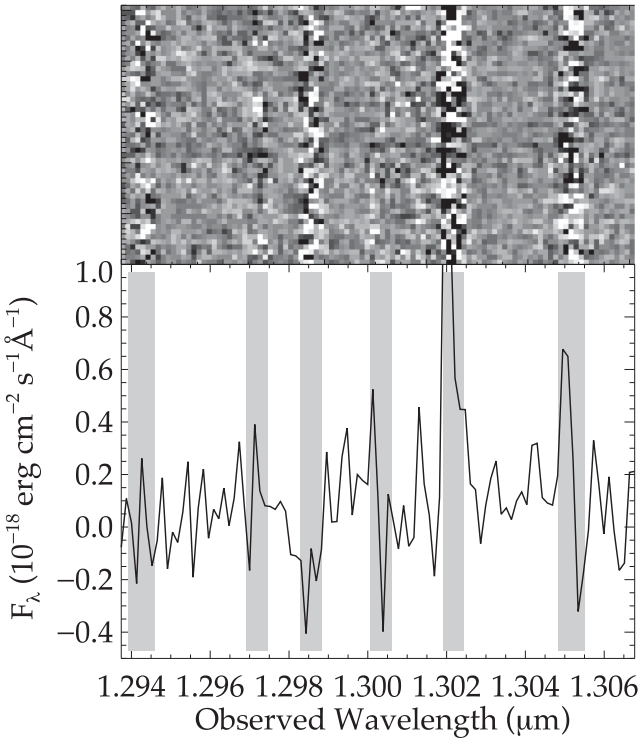

Figure 3. Non-detection of [C III] λ1907, C III] λ1909 doublet in a Keck/MOSFIRE *J*-band spectrum of the spectroscopically confirmed $z = 5.828$ galaxy A1703-23 (see Section 3.4 for details). Top panel shows the two-dimensional (unsmoothed) spectra with black corresponding to positive emission. The one-dimensional extracted spectra are shown in the lower panel. Vertical grey swaths indicate regions of elevated noise from OH skylines. Based on the Lyα redshift, [C III] λ1907 is expected to lie between 1.2999 and 1.3019 μm, and C III] λ1909 should be located between 1.3013 and 1.3033 μm.

velocity offsets of 360–430 km s^{-1}. If we conservatively assume an FWHM of 10 Å (roughly two times as large as the unresolved C IV line in A1703-zd6), we find that the 5σ flux limit remains fairly low (3.2–3.9 $\times$ 10^{-18} erg cm^{-2} s^{-1}) in this region. Considering the entire spectral window over which [C III] λ1907 is expected, we find that the median 5σ limit on the line flux is 3.5 $\times$ 10^{-18} erg cm^{-2} s^{-1}. Roughly 70 per cent of the C III] λ1909 spectral window is clean with a 5σ flux limit of 5.6 $\times$ 10^{-18} erg cm^{-2} s^{-1}. The C III] λ1909 flux limit is slightly larger because the adopted 10 Å line width overlaps with the OH line. Applying an aperture correction of a factor of 1.66 (calculated from the seeing, slit width, and source size), we derive 5σ rest-frame equivalent width limits of 2.7 Å for [C III] λ1907 and 4.3 Å for C III] λ1909. Detection of both components of the doublet would require a total equivalent width in excess of 7.0 Å.

While of course there is some possibility that the line might have been obscured by a skyline, we note that the non-detection of C III] in A1703-23 is consistent with the physical picture presented in Stark et al. (2014). At intermediate redshifts, the C III] equivalent width is found to increase with the Lyα equivalent width. For galaxies with Lyα equivalent widths similar to the moderate value observed in A1703-23, C III] rest-frame equivalent widths are seen to be in the range $W_{\rm C\,III]} \simeq$ 2–4 Å (Shapley et al. 2003; Stark et al. 2014), below the equivalent width limit provided by the MOSFIRE spectrum. However, recent studies have demonstrated that some galaxies at $z \simeq$ 6–7 have UV metal lines that are stronger than found in the intermediate-redshift samples. The non-detection of C III] in A1703-23 suggests that not all $z \gtrsim 6$ galaxies have such extreme rest-UV spectra.

4 A HARD IONIZING SPECTRUM AT $z = 7$

Here we use photoionization models to characterize the shape of the ionizing spectrum required to produce the observed spectral properties of A1703-zd6. We explore galaxy models with stellar input spectra in Section 4.1 and AGN models in Section 4.2.

4.1 Stellar models

We fit the observed C IV λ1548 emission equivalent width (the component of the doublet that is most robustly detected) and broad-band *F*125*W* and *F*160*W* fluxes of the galaxy using an approach similar to that adopted in Stark et al. (2014). This is based on a combination of the latest version of the Bruzual & Charlot (2003) stellar population synthesis model with the standard photoionization code CLOUDY (Ferland et al. 2013) to describe the emission from stars and the interstellar gas (Gutkin et al., in preparation, who follow the prescription of Charlot & Longhetti 2001). The Gutkin et al. models include the latest developments in the modelling of stellar interiors and atmospheres included in the Bruzual–Charlot software (Charlot & Bruzual, in preparation) and incorporate the evolutionary tracks of Chen et al. (2015) for massive stars. Additional details can be found in Stark et al. (2014).

We adopt the same parametrization of interstellar gas and dust as in Stark et al. (2015), to whom we refer for detail. In brief, the main adjustable parameters of the photoionized gas are the interstellar metallicity, *Z*, the typical ionization parameter of a newly ionized H II region, *U* (which characterizes the ratio of ionizing photon to gas densities at the edge of the Strömgren sphere), and the dust-to-metal (mass) ratio, $\xi_{\rm d}$ (which characterizes the depletion of metals on to dust grains). We consider here models with hydrogen densities ranging between 100 and 1000 cm^{-3} and C/O (and N/O) abundance ratios ranging from 1.0 to 0.1 times the standard values in nearby galaxies [$(\rm C/O)_\odot \approx 0.44$ and $(\rm N/O)_\odot \approx 0.07$]. We also include attenuation of line and continuum photons by dust in the neutral ISM, using the two-component model of Charlot & Fall (2000), as implemented by da Cunha, Charlot & Elbaz (2008, their equations 1–4). This is parametrized in terms of the total *V*-band attenuation optical depth of the dust, $\hat{\tau}_V$, and the fraction μ of this arising from dust in the diffuse ISM rather than in giant molecular clouds. Accounting for these two dust components is important to describe the different attenuation of emission line and stellar continuum photons. We use a comprehensive model grid similar to that adopted by Stark et al. (2015). The values reported for each quantity in Table 3 are the median and 16–84 per cent percentile range of the probability density function obtained from the Bayesian analysis described in this section. The 'best-fitting' values correspond to the model producing the minimum χ^2.

As in Stark et al. (2015), we consider models with two-component star formation histories: a 'starburst' component (represented here by a 3-Myr-old stellar population with constant SFR) and an 'old' component (represented by a stellar population with constant or exponentially declining SFR with age between 10 Myr and the age of the Universe at the galaxy redshift, i.e. 0.75 Gyr). We adopt a standard Chabrier (2003) initial mass function and the same stellar metallicity for both components, which also coincides with the current interstellar metallicity of the galaxy.

To interpret the combined stellar and nebular emission from the galaxy, we use the same Bayesian approach as in Stark et al. (2015,

Table 3. A1703-zd6 photoionization modelling results. The input spectra to the photoionization code are from the latest version of the Bruzual & Charlot (2003) stellar population synthesis models. We fit the C IV λ1548 equivalent width and J_{125} and H_{160} broad-band flux densities.

A1703-zd6	
$\log U$	$-1.35^{+0.24}_{-0.39}$
$12 + \log(\mathrm{O/H})$	$7.04^{+0.31}_{-0.25}$
$\log(\xi_{\mathrm{ion}}/\mathrm{Hz\,erg^{-1}})$	$25.68^{+0.27}_{-0.19}$
$\log[W(\mathrm{Ly}\alpha)/\text{Å}]$	$2.06^{+0.33}_{-0.23}$
log(N IV 1486/C IV 1548)	$-1.93^{+0.32}_{-0.18}$
log(N V 1240/C IV 1548)	$-2.44^{+0.42}_{-0.42}$
log(He II 1640/C IV 1548)	$-1.59^{+0.22}_{-0.20}$

see also equation 2.10 of Pacifici et al. 2012) and a grid of models covering wide ranges in the above parameters. In practice, we find that the requirement to reproduce the strong C IV λ1548 emission equivalent width implies that the best-fitting models are entirely dominated by the young stellar component (for reference, the best-fitting model rest-frame equivalent width for this line is 19.9 Å). Such models also provide excellent fits to the observed *F*125*W* and *F*160*W* fluxes (with a dust attenuation optical depth consistent with zero). Also, since nebular emission is constrained only by the equivalent width of a single component of the C IV doublet in our analysis, the resulting constraints on the gas density and C/O ratio are extremely weak.

The models demonstrate that the C IV emission line strength of A1703-zd6 can be reproduced by stellar input spectra. The range of acceptable model parameters is shown in Table 3. Models that fit the observed spectral properties have a large ionization parameter ($\log U = -1.35$) and very low metallicity ($12 + \log \mathrm{O/H} = 7.05$). The production rate of hydrogen ionizing photons per observed (i.e. attenuated) 1500 Å luminosity is very large ($\log(\xi_{\mathrm{ion}}/\mathrm{erg^{-1}\,Hz}) = 25.68$) in models that reproduce the data. We note that we do not attenuate the ionizing photon output in our calculation of ξ_{ion}, as our primary goal is to be able to predict how many hydrogen ionizing photons were produced based on the observed 1500 Å luminosity.

The ionizing spectrum of the best-fitting stellar model (Fig. 4) reveals a significant flux of energetic radiation at 40–50 eV capable of producing nebular C IV emission. The flux density drops off significantly above ∼54 eV, resulting in much weaker emission from He II and N V. Stellar models predict N V λ1240 and He II λ1640 fluxes that are 30–250 times weaker than the C IV λ1548 line strength (Table 3). These lines are unlikely to be detected if the C IV emission is powered by a stellar population.

4.2 AGN models

We also explore a comparison of A1703-zd6 to AGN photoionization models. We use the models of Feltre et al. (in preparation), which represent the narrow-line emission region (NLR) of the AGN and have been realized with the photoionization code CLOUDY (latest version C13.03, last described in Ferland et al. 2013). The solar abundance and dust depletion values are the same as those used in the models for star-forming galaxies used in Section 4.1 and developed by Gutkin et al. (in preparation). The input parameters for the AGN NLR models are taken to be the interstellar metallicity, *Z*, in the range between 0.0001 and 0.05, the dust-to-metal (mass) ratio,

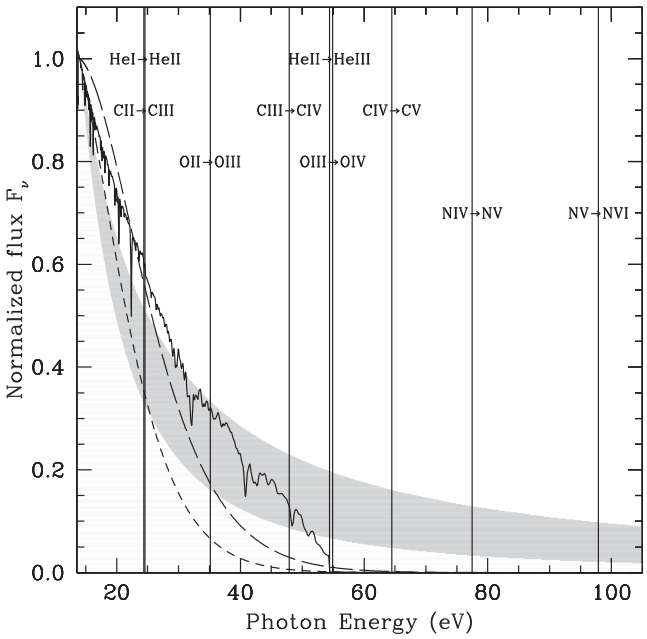

Figure 4. Ionizing spectra from different sources, plotted together with the ionizing potentials of different ions (vertical lines). The solid spectral energy distribution corresponds to the best-fitting galaxy model reported in Section 4, while the shaded area shows the range in ionizing spectra produced by $F_\nu \propto \nu^\alpha$ AGN models with spectral indices between $\alpha = 1.2$ (upper ridge) and 2.0 (lower ridge). For comparison to the radiation field in typical galaxies at $z \simeq 2$ (Steidel et al. 2014), we also display blackbody spectra with temperatures of 45 000 (short dashed) and 55 000 K (long dashed), respectively. All spectra are normalized to unity at 13.6 eV.

$\xi_{\mathrm{d}} = 0.1$, 0.3 and 0.5, the hydrogen density, $n_{\mathrm{H}} = 10^2$, 10^3 and 10^4 cm^{-3}, and the ionization parameter, *U*, in the range $\log U = -5$ to -1. The AGN is characterized by a power law $F_\nu \propto \nu^\alpha$, with spectral indices $\alpha = -1$, 2, -1.4, -1.7 and -2.0 in the wavelength range between 0.001 and 0.25 μm. For completeness, we include the effects of attenuation using the prescription of Calzetti et al. (2000).

In contrast to the stellar model fits (Section 4.1), we do not include the constraints from the line equivalent widths and broad-band photometry because of the arbitrary scaling of the AGN and host galaxy luminosities that would be required to model the underlying continuum. The AGN fit is instead focused on the two most robustly constrained flux ratios, namely O III](1661)/C IV(1548) and He II(1640)/C IV(1548). Given the tentative nature of the O III] λ1661 detection, we adopt a 5σ upper limit ($<3.5 \times 10^{-18}$ erg cm^{-2} s^{-1}) to the line flux. We note that this limit is consistent with the observed faint flux level of the possible emission feature (1.8×10^{-18} erg cm^{-2} s^{-1}). The measurement of C IV λ1548 and upper limits on O III] λ1661 and He II thus translate into upper limits for the emission line ratios O III] λ1661/C IV λ1548 and He II/C IV λ1548 used in the fit.

The fitting procedure demonstrates that the existing observational constraints are also marginally consistent with photoionization by an AGN. The two flux ratio limits favour best-fitting AGN models corresponding to metallicity and hydrogen density of $Z = 0.001$ and 10^2 cm^{-3}, respectively. The ionizing spectra of acceptable AGN models are shown in Fig. 4. The AGN power-law spectrum has considerably greater flux than the galaxy models at energies in excess of 50 eV. As a result, AGN models predict stronger He II λ1640 than the galaxy models discussed in Section 4.2, with a flux

that is 40 per cent that of the measured C IV λ1548 flux. Current limits suggest that the He II flux is less than 50 per cent that of C IV λ1548 at 2σ. Deeper *J*-band observations may thus be able to detect He II if A1703-zd6 is powered by an AGN.

5 DISCUSSION

5.1 Comparison to UV radiation field at lower redshifts

Nebular C IV emission is seldom detected in $z \simeq 2$–3 galaxies. Instead, the C IV profile shows strong absorption from highly ionized outflowing gas superimposed on a P-Cygni profile from stellar winds (e.g. Shapley et al. 2003). The absence of strong C IV emission in typical galaxies points to a negligible output of photons with energies greater than 47.9 eV, consistent with the radiation field expected from the blackbody models predicted for $z \simeq 2$ galaxies in Steidel et al. (2014). In Fig. 4, we overlay the $z \simeq 2$ galaxy ionizing spectrum on the AGN and stellar photoionization models which reproduce the spectral features of A1703-zd6. Both models predict that the $z = 7.045$ galaxy must have a larger output of 20–50 eV radiation than is commonly seen in $z \simeq 2$–3 galaxies.

When strong C IV emission is present in lower redshift systems, it is generally thought to reflect AGN activity. At $z \simeq 2$–3, AGNs with narrow emission lines (FWHM less than 2000 km s^{-1}) comprise only 1 per cent of UV-selected galaxy samples (Steidel et al. 2002; Hainline et al. 2011). In these systems, the C IV flux is typically 20 per cent that of Lyα, with rest-frame equivalent widths ranging between 10 and 50 Å (Steidel et al. 2002; Hainline et al. 2011; Alexandroff et al. 2013), comparable to what is observed in A1703-zd6 (Fig. 5). Nebular He II is often seen in UV-selected narrow-lined AGNs, but the rest-frame equivalent width is only 5–10 Å (Hainline et al. 2011), also consistent with the non-detection of He II in A1703-zd6. While the line properties of A1703-zd6 and UV-selected AGNs appear similar, the continuum shapes are very different. Hainline et al. (2011) demonstrated that at lower redshift, the UV continuum power-law slope of the UV-selected AGNs ($\beta = -0.3$) tends to be much redder than non-AGNs ($\beta = -1.5$). In contrast, A1703-zd6 has a very blue ($\beta = -2.4$) continuum slope (Bradley et al. 2012; Schenker et al. 2012), similar to the parent population of galaxies at $z \simeq 7$ (e.g. Bouwens et al. 2014).

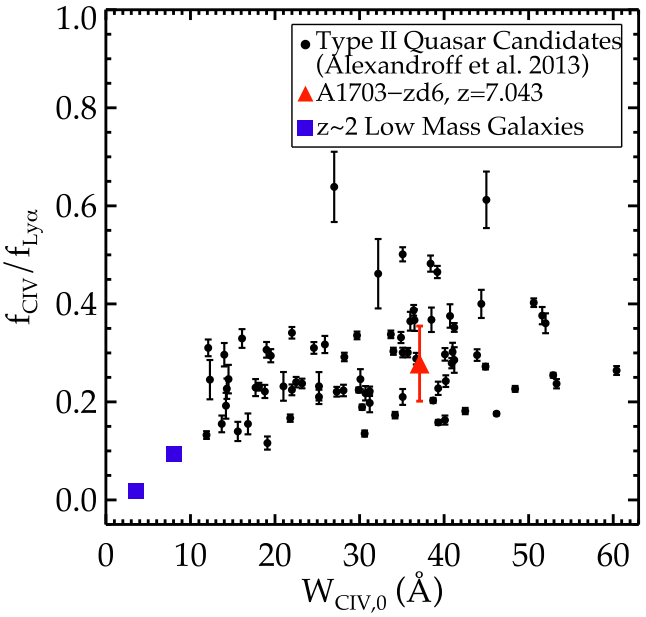

Figure 5. Comparison of the C IV/Lyα flux ratio in A1703-zd6 with type II quasar candidates at $2 < z < 4.3$ and low-mass metal-poor galaxies at $z \simeq 2$. The quasar candidates were reported in Alexandroff et al. (2013) and the low-mass $z \simeq 2$ galaxies are C IV emitters from Stark et al. (2014). The C IV emitting strength of A1703-zd6 is comparable to that seen in AGN spectra and is more extreme than in powerful line emitting galaxies at lower redshift.

Among star-forming galaxies with low stellar masses (10^6–10^9 M$_\odot$), nebular C IV emission is more common (Christensen et al. 2012; Stark et al. 2014). These systems tend to have blue colours, large specific star formation rates and prominent Lyα emission lines. The strong C IV emission is thought to reflect an intense radiation field from massive stars following a recent upturn in star formation (Stark et al. 2014). Given the similarly low masses, blue colours and large specific star formation rates of reionization-era galaxies, it is possible that nebular C IV emission might be more common in $z > 6$ galaxies. Yet as is evident in Fig. 5, the C IV equivalent widths and C IV/Lyα flux ratios of A1703-zd6 are 5–10 times larger than the low-mass samples at lower redshift. The offset from the $z \simeq 2$ galaxy population remains if we adopt the lower limit on the C IV λ1550 flux (see Section 3.1). In this case, the C IV/Lyα flux ratio is 0.2 and the total C IV rest-frame equivalent width is 30 Å, both consistent with the narrow-lined AGNs shown in Fig. 5. We note that the increased C IV/Lyα flux ratio of A1703-zd6 with respect to $z \simeq 2$ systems could be in part due to suppression of Lyα emission by the IGM or optically thick absorbers. But given the very large rest-frame Lyα equivalent width of this system (65 Å; Schenker et al. 2012), IGM attenuation is not likely to be the primary factor responsible for the nearly order of magnitude offset in the C IV/Lyα ratio compared to the lower redshift systems.

There does not appear to be a completely analogous population to A1703-zd6 at lower redshift. Deeper spectroscopic constraints on other ultraviolet spectral features (N V, He II, C III]) will help characterize the powering mechanism. Another crucial step will be determining whether systems like A1703-zd6 are common at $z \simeq 7$. The only other galaxy in our sample with a redshift which places C IV in the spectral window we targeted is A1703-zd1a (Section 3.2). The non-detection of C IV in this system suggests that the line is not strong in all $z \simeq 7$ galaxies. But the presence of nebular C IV emission in one of two galaxies we observed represents a significant departure from the 1 per cent detection rate at lower redshift. If the galaxies in our sample are typical of the UV-selected population at $z \simeq 7$, it would suggest that a very different UV radiation field is present in many early star-forming systems, potentially altering our current picture of the contribution of galaxies to reionization (e.g. Bouwens et al. 2015; Robertson et al. 2015). If the duty cycle associated with the intense radiation field is large (such that A1703-zd6 is not a bursty outlier), then it would be possible to achieve reionization by $z \simeq 6$ while adopting a lower ionizing photon escape fraction (f_{esc}) or a brighter absolute magnitude limit when integrating the UV luminosity function.

5.2 Nature of $z > 7$ Lyα emitters

Currently all $z > 7$ UV metal line detections come from galaxies with previously known Lyα detections. This largely reflects our selection criteria, as we have primarily focused our follow-up on known Lyα emitters. The spectroscopic redshifts provided by Lyα are very useful, allowing us to ensure that UV metal lines are located at wavelengths which are unobscured by the atmosphere. But given the unusually strong C IV emission, we must consider whether our

pre-selection of Lyα emitters might have biased us towards locating galaxies with extreme radiation fields.

While Lyα emission is very common among $z \simeq 6$ galaxies (Stark et al. 2011), it is exceedingly rare at $z \simeq 7$ (e.g. Treu et al. 2013; Schenker et al. 2014; Tilvi et al. 2014). The weak Lyα emission is thought to reflect an increase in the IGM neutral hydrogen fraction over $6 < z < 8$ (Choudhury et al. 2014; Mesinger et al. 2015), as would be expected if reionization is incomplete at $z \simeq 7$–8 (e.g. Robertson et al. 2013, 2015). Recent work suggests that an increased incidence of optically thick absorbers may also contribute to the attenuation of Lyα (Bolton & Haehnelt 2013), although the importance of such systems remains unclear (Mesinger et al. 2015). Based on this overall picture, galaxies with Lyα detections at $z > 7$, such as A1703-zd6, will be those that are situated in regions of the IGM which have already been ionized.

It is conceivable that the only $z > 7$ galaxies that can be seen in Lyα are those with extreme radiation fields capable of ionizing hydrogen in the IGM and in optically thick absorbers. In this case, the presence of high-ionization features like C IV in A1703-zd6 would be a direct consequence of the pre-selection by Lyα. Given the rarity of Lyα emitters at $z > 7$, the hard ionizing spectrum shown in Fig. 4 would thus be limited to a small percentage of the early galaxy population. Additional constraints on the strength of high-ionization lines in $z > 7$ Lyα emitters will be needed to determine whether the presence of Lyα is indeed linked to the intensity of the radiation field. Likewise, determination of the typical ionizing spectrum will require sampling galaxies with a diverse range of properties, including those without Lyα emission.

5.3 Implications for early galaxy spectroscopy

Recent studies have proposed that the [C III] λ1907, C III] λ1909 doublet provides a feasible route towards spectroscopic confirmation of reionization-era galaxies in which Lyα is strongly attenuated by the partially neutral IGM (Erb et al. 2010; Stark et al. 2014). The line may provide a valuable spectroscopic probe of the most distant galaxies that the *JWST* will find, as the strong rest-optical lines shift out of the spectral window of NIRSPEC at $z \simeq 11$. For future ground-based optical/infrared telescopes, C III] may be brightest spectral lines in reionization-era systems. But because of atmospheric absorption in the NIR, ground-based facilities will not be able to detect C III] emission throughout substantial redshift intervals in the reionization era. In Fig. 6, we show the redshift ranges over which various UV emission lines fall into the *Y*, *J*, *H* and K_s bands of MOSFIRE. C III] is not visible for galaxies with redshifts $6.0 < z < 6.7$ and $8.5 < z < 9.4$. The redshift range over which C III] is significantly attenuated by the atmosphere is somewhat larger, spanning $5.8 \lesssim z \lesssim 6.9$ and $8.3 \lesssim z \lesssim 10$, respectively.

The presence of C IV and tentative identification of O III] in A1703-zd6 suggests that a variety of FUV lines may be present in deep NIR spectra of a subset of bright $z > 6$ galaxies. While it is possible that A1703-zd6 may have atypically strong C IV emission (see Section 5.2), both C IV and O III] emission are commonly detected in the spectra of intermediate-redshift metal-poor galaxies (Erb et al. 2010; Christensen et al. 2012; Stark et al. 2014). Importantly, both lines are detectable at redshifts where C III] is unobservable. C IV can be seen in galaxies over $6.4 < z < 7.7$ (*J* band) and $8.5 < z < 10.7$ (*H* band), while O III] can be identified in galaxies at $5.9 < z < 7.1$ and $7.8 < z < 9.8$ (Fig. 6).

The redshift-dependent visibility of the FUV metal lines shown in Fig. 6 has implications for the optimal strategy of spectroscopically following up early star-forming systems. Of particular interest is the population of extreme [O III]+Hβ emitting galaxies identified via blue [3.6]−[4.5] colours (Smit et al. 2014, 2015) and thought to lie in the redshift range $z \simeq 6.6$–6.9. Stark et al. (2014) demonstrate that galaxies with extreme optical line emission tend to have large equivalent width FUV metal lines (see Gutkin et al., in preparation, for more details), making this an attractive class of objects to target with rest-frame FUV spectroscopy. However, Fig. 6 demonstrates that C III] is likely to be obscured by the atmosphere over some of this redshift range. For the same reason, attempts to identify C III] emission in Lyα emitters at $z = 6.6$ will not result in many detections. Follow-up efforts of both populations are more likely to succeed by focusing on C IV, He II and O III] in the *J* band.

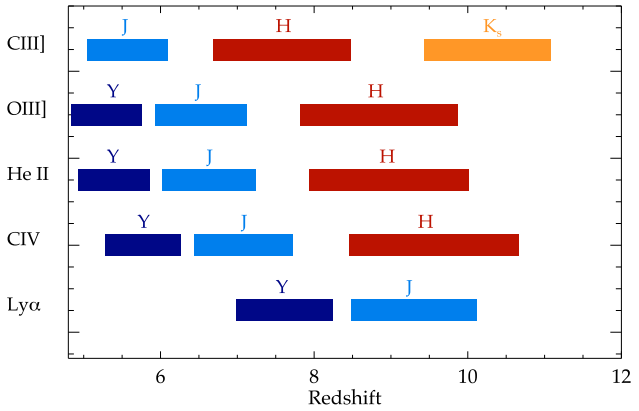

Figure 6. Visibility of FUV lines in $z > 5$ galaxies using ground-based spectrographs. Solid bands give redshift window over which emission lines are detectable in *Y*, *J*, *H* and K_s-band filters using MOSFIRE on Keck. Atmospheric absorption in the NIR limits the redshift range over which any individual spectral feature can be detected.

6 SUMMARY

We have presented new measurements of various FUV emission lines (Lyα, C IV, He II, O III]) in $z \sim 6$–8 galaxy spectra. Using the MOSFIRE spectrograph (McLean et al. 2012) on Keck I, we have obtained *J*-band spectra of four gravitationally lensed galaxies in the massive cluster field Abell 1703 (Table 1). The galaxies are bright ($H = 23.8$–25.9) and span a range of redshifts ($5.8 \lesssim z \lesssim 8.0$), Ly$\alpha$ equivalent widths, UV slopes and continuum luminosities.

We report a 6.8σ detection of nebular C IV λ1548 emission in A1703-zd6, a $z = 7.045$ spectroscopically confirmed galaxy. The observed wavelengths of the UV metal lines are accurately known from the Lyα redshift. The rest-frame C IV equivalent width and C IV/Lyα flux ratio we infer for A1703-zd6 are similar to those seen in narrow-lined AGNs at lower redshift. The line is unresolved with an FWHM less than 125 km s^{-1}. The presence of C IV requires a surprisingly large output of very energetic radiation capable of triply ionizing carbon. In Section 4, we demonstrated that the extreme spectral properties of A1703-zd6 can be powered by an AGN or an intense population of young, very hot, metal-poor stars. Photoionization models point to an ionizing spectrum that is very different from that inferred for typical $z \simeq 2$ galaxies.

The data provide constraints on UV metal line emission in two other galaxies. The first of these is A1703-zd1a, a *z*-band dropout thought to lie at $z \simeq 6.6$–6.9 (Smit et al. 2014). In this redshift range, the MOSFIRE observations probe C IV, He II and O III]. No secure emission lines are identified throughout the *J*-band spectrum. Rest-frame equivalent widths greater than 2.3 Å would have been

seen at 5σ if located between OH skylines. The other system is A1703-23, a spectroscopically confirmed galaxy at $z = 5.828$. We report an upper limit of 2.7 Å on [C III] λ1907 and 4.3 Å on C III] λ1909 emission, provided the line is not obscured by skylines. The lack of detectable C III] emission is consistent with the relationship between C III] and Lyα equivalent width presented in Stark et al. (2014).

At lower redshift, nebular C IV emission is seen in only 1 per cent of UV-selected galaxies (Steidel et al. 2002; Hainline et al. 2011). The presence of strong C IV emission in A1703-zd6, one of the first galaxies we targeted, is thus rather surprising. One explanation is that radiation fields are more extreme in $z \simeq 7$ galaxies. This may be expected if reionization-era galaxies are commonly caught following a recent upturn or burst of star formation and would indicate that $z > 7$ systems are more efficient ionizing agents than we previously thought. Alternatively, we consider whether the only systems seen in Lyα at $z > 7$ may be those with extreme radiation fields capable of ionizing hydrogen in optically thick absorbers and the surrounding IGM. In this case, the pre-selection of galaxies by their Lyα emission would result in a very biased sample with extreme spectral features. Further constraints on high-ionization emission lines in galaxies with and without Lyα should clarify whether systems like A1703-zd6 are ubiquitous at $z > 7$.

ACKNOWLEDGEMENTS

We thank Richard Ellis, Dawn Erb, Martin Haehnelt, Juna Kollmeier, Ian McGreer and Andrei Mesinger for enlightening conversations. DPS acknowledges support from the National Science Foundation through the grant AST-1410155. JR acknowledges support from the European Research Council (ERC) starting grant CALENDS and the Marie Curie Career Integration Grant 294074. SC, JG and AW acknowledge support from the ERC via an Advanced Grant under grant agreement no. 321323 – NEOGAL. This work was partially supported by a NASA Keck PI Data Award, administered by the NASA Exoplanet Science Institute. Data presented herein were obtained at the W. M. Keck Observatory from telescope time allocated to the National Aeronautics and Space Administration through the agency's scientific partnership with the California Institute of Technology and the University of California. The Observatory was made possible by the generous financial support of the W. M. Keck Foundation. We acknowledge the very significant cultural role that the summit of Mauna Kea has always had within the indigenous Hawaiian community. We are most fortunate to have the opportunity to conduct observations from this mountain.

REFERENCES

Alexandroff R. et al., 2013, MNRAS, 435, 3306
Atek H. et al., 2011, ApJ, 743, 121
Atek H. et al., 2015, ApJ, 800, 18
Bayliss M. B., Rigby J. R., Sharon K., Wuyts E., Florian M., Gladders M. D., Johnson T., Oguri M., 2014, ApJ, 790, 144
Bolton J. S., Haehnelt M. G., 2013, MNRAS, 429, 1695
Bouwens R. J. et al., 2014, ApJ, 793, 115
Bouwens R. J. et al., 2015, ApJ, 803, 34
Bowler R. A. A. et al., 2014, preprint (arXiv:e-prints)
Bradley L. D. et al., 2012, ApJ, 747, 3
Bradley L. D. et al., 2014, ApJ, 792, 76
Bruzual G., Charlot S., 2003, MNRAS, 344, 1000
Calzetti D., Armus L., Bohlin R. C., Kinney A. L., Koornneef J., Storchi-Bergmann T., 2000, ApJ, 533, 682
Chabrier G., 2003, PASP, 115, 763
Charlot S., Fall S. M., 2000, ApJ, 539, 718
Charlot S., Longhetti M., 2001, MNRAS, 323, 887
Chen Y., Bressan A., Girardi L., Marigo P., Kong X., Lanza A., 2015, MNRAS, 452, 1068
Choudhury T. R., Puchwein E., Haehnelt M. G., Bolton J. S., 2014, preprint (arXiv:1412.4790)
Christensen L. et al., 2012, MNRAS, 427, 1953
Coe D. et al., 2013, ApJ, 762, 32
Curtis-Lake E. et al., 2012, MNRAS, 422, 1425
Curtis-Lake E. et al., 2014, preprint (arXiv:1409.1832)
da Cunha E., Charlot S., Elbaz D., 2008, MNRAS, 388, 1595
Duncan K. et al., 2014, MNRAS, 444, 2960
Ellis R. S. et al., 2013, ApJ, 763, L7
Erb D. K., Pettini M., Shapley A. E., Steidel C. C., Law D. R., Reddy N. A., 2010, ApJ, 719, 1168
Ferland G. J. et al., 2013, Rev. Mex. Astron. Astrofis., 49, 137
Finkelstein S. L. et al., 2012, ApJ, 756, 164
Garnett D. R., Skillman E. D., Dufour R. J., Peimbert M., Torres-Peimbert S., Terlevich R., Terlevich E., Shields G. A., 1995, ApJ, 443, 64
Garnett D. R., Skillman E. D., Dufour R. J., Shields G. A., 1997, ApJ, 481, 174
Garnett D. R., Shields G. A., Peimbert M., Torres-Peimbert S., Skillman E. D., Dufour R. J., Terlevich E., Terlevich R. J., 1999, ApJ, 513, 168
González V., Bouwens R., Illingworth G., Labbé I., Oesch P., Franx M., Magee D., 2014, ApJ, 781, 34
Grazian A. et al., 2015, A&A, 575, A96
Hainline K. N., Shapley A. E., Kornei K. A., Pettini M., Buckley-Geer E., Allam S. S., Tucker D. L., 2009, ApJ, 701, 52
Hainline K. N., Shapley A. E., Greene J. E., Steidel C. C., 2011, ApJ, 733, 31
Hashimoto T., Ouchi M., Shimasaku K., Ono Y., Nakajima K., Rauch M., Lee J., Okamura S., 2013, ApJ, 765, 70
James B. L. et al., 2014, MNRAS, 440, 1794
Kewley L. J., Maier C., Yabe K., Ohta K., Akiyama M., Dopita M. A., Yuan T., 2013, ApJ, 774, L10
Labbé I. et al., 2013, ApJ, 777, L19
McLean I. S. et al., 2012, Proc. SPIE, 8446, 84460J
McLinden E. M. et al., 2011, ApJ, 730, 136
McLure R. J. et al., 2013, MNRAS, 432, 2696
Maseda M. V. et al., 2014, ApJ, 791, 17
Mesinger A., Aykutalp A., Vanzella E., Pentericci L., Ferrara A., Dijkstra M., 2015, MNRAS, 446, 566
Oesch P. A. et al., 2010, ApJ, 709, L21
Oesch P. A. et al., 2014, ApJ, 786, 108
Oke J. B., Gunn J. E., 1983, ApJ, 266, 713
Ono Y. et al., 2013, ApJ, 777, 155
Pacifici C., Charlot S., Blaizot J., Brinchmann J., 2012, MNRAS, 421, 2002
Richard J., Pei L., Limousin M., Jullo E., Kneib J. P., 2009, A&A, 498, 37
Robertson B. E. et al., 2013, ApJ, 768, 71
Robertson B. E., Ellis R. S., Furlanetto S. R., Dunlop J. S., 2015, ApJ, 802, L19
Rogers A. B., McLure R. J., Dunlop J. S., 2013, MNRAS, 429, 2456
Salmon B. et al., 2015, ApJ, 799, 183
Schenker M. A., Stark D. P., Ellis R. S., Robertson B. E., Dunlop J. S., McLure R. J., Kneib J.-P., Richard J., 2012, ApJ, 744, 179
Schenker M. A. et al., 2013a, ApJ, 768, 196
Schenker M. A., Ellis R. S., Konidaris N. P., Stark D. P., 2013b, ApJ, 777, 67
Schenker M. A., Ellis R. S., Konidaris N. P., Stark D. P., 2014, ApJ, 795, 20
Shapley A. E., Steidel C. C., Pettini M., Adelberger K. L., 2003, ApJ, 588, 65
Shim H., Chary R.-R., Dickinson M., Lin L., Spinrad H., Stern D., Yan C.-H., 2011, ApJ, 738, 69
Smit R., Bouwens R. J., Franx M., Illingworth G. D., Labbé I., Oesch P. A., van Dokkum P. G., 2012, ApJ, 756, 14
Smit R. et al., 2014, ApJ, 784, 58
Smit R. et al., 2015, ApJ, 801, 122

Stark D. P., Ellis R. S., Ouchi M., 2011, ApJ, 728, L2
Stark D. P., Schenker M. A., Ellis R., Robertson B., McLure R., Dunlop J., 2013, ApJ, 763, 129
Stark D. P. et al., 2014, MNRAS, 445, 3200
Stark D. P. et al., 2015, MNRAS, 450, 1846
Steidel C. C., Hunt M. P., Shapley A. E., Adelberger K. L., Pettini M., Dickinson M., Giavalisco M., 2002, ApJ, 576, 653
Steidel C. C., Erb D. K., Shapley A. E., Pettini M., Reddy N., Bogosavljević M., Rudie G. C., Rakic O., 2010, ApJ, 717, 289
Steidel C. C. et al., 2014, ApJ, 795, 165
Tapken C., Appenzeller I., Noll S., Richling S., Heidt J., Meinköhn E., Mehlert D., 2007, A&A, 467, 63
Tilvi V. et al., 2014, ApJ, 794, 5
Treu T., Schmidt K. B., Trenti M., Bradley L. D., Stiavelli M., 2013, ApJ, 775, L29
van der Wel A. et al., 2011, ApJ, 742, 111
Vanzella et al., 2010, A&A, 513, 20
Wilkins S. M., Bunker A. J., Stanway E., Lorenzoni S., Caruana J., 2011, MNRAS, 417, 717
Zheng W. et al., 2009, ApJ, 697, 1907
Zheng W. et al., 2012, Nature, 489, 406
Zitrin A. et al., 2014, ApJ, 793, L12

This paper has been typeset from a TEX/LATEX file prepared by the author.